

Activation and Detection of Facilitation as Studied by Presynaptic Voltage Control at the Inhibitor of the Crayfish Opener Muscle

ANDREY VYSHEDSKIY AND JEN-WEI LIN

Department of Biology, Boston University, Boston, Massachusetts 02215

Vyshedskiy, Andrey and Jen-Wei Lin. Activation and detection of facilitation as studied by presynaptic voltage control at the inhibitor of the crayfish opener muscle. *J. Neurophysiol.* 77: 2300–2315, 1997. Facilitation at the crayfish neuromuscular inhibitor synapse was investigated with the use of a presynaptic voltage control method in which 5-ms presynaptic pulses were used to activate and monitor facilitation. A single 5-ms pulse was able to activate facilitation with a decay time constant similar to that of the F2 component of facilitation activated by action potentials. The quality of the control of presynaptic potential during F2 facilitation was evaluated by measuring the amplitude of presynaptic pulses and by analyzing the shape of the depolarization-release coupling plot during facilitation. Both approaches suggested that neither the amplitude of presynaptic depolarizations nor the space clamp of the presynaptic axon was changed during F2 facilitation. The activation of facilitation was examined by changing the amplitude of conditioning pulses systematically and using a test pulse of a constant amplitude to monitor facilitation. We found that a significant amount of facilitation could be activated by conditioning pulses that were subthreshold to the activation of transmitter release. Facilitation plateaued before the inhibitory postsynaptic potentials (IPSPs) activated by conditioning pulses reached their maximum. A double logarithm plot of facilitation magnitude against the conditioning IPSP amplitude yielded a slope of 0.34, which implies that the calcium ion cooperativity of activating facilitation is about one third of the secretion process. These findings enabled us to activate near maximal facilitation, by a burst of subthreshold conditioning pulses, without any conditioning transmitter release, and, therefore, to avoid complications associated with previous transmitter release. The detection of facilitation was examined by changing test pulse amplitude systematically to evaluate the ability of the test pulse to detect a constant level of facilitation. The magnitude of normalized facilitation decreased with increasing test pulse amplitude. The magnitude of absolute facilitation (the amplitude of the facilitated minus the control IPSP) increased with increasing test pulse amplitude. A double logarithm plot between facilitated and control IPSPs gave rise to a slope of 0.77, which suggests that the calcium cooperativity of transmitter release was decreased during facilitation.

INTRODUCTION

Synaptic facilitation is a widely observed form of synaptic plasticity. Facilitation is classified under the category of short-term synaptic enhancement, which includes the F1 and F2 components of facilitation, augmentation, and posttetanic potentiation (Magleby 1987). These short-term plastic components are able to increase the strength of synaptic transmission for different durations. The F1 and F2 components decay with a time constant of tens and hundreds of milliseconds, respectively. Augmentation and posttetanic potentiation are longer lasting, with decay time constants of ~3–10 and ~30–90 s, respectively. The kinetics of the F2 com-

ponent and augmentation can be specifically modified by replacing extracellular calcium with strontium and by adding 0.1–0.2 mM barium to physiological saline (Quastel and Saint 1988; Zengel and Magleby 1980). These distinctions suggest that the individual components could be mediated by separate molecular mechanisms.

The earliest hypothesis to explain synaptic facilitation is the classical residual calcium hypothesis originated from studies at the frog neuromuscular junction (Dodge and Rahamimoff 1967; Katz and Miledi 1968; Martin 1977). This hypothesis has been extensively evaluated and revised by kinetic analysis and mathematical modeling (Bertram et al. 1996; Magleby 1987; Stanley 1986; Winslow et al. 1994; Yamada and Zucker 1992; Zucker and Stockbridge 1983). Calcium imaging studies, although confirming the importance of intracellular free calcium ions ($[Ca^{2+}]_i$) in synaptic enhancement, showed that the classical model cannot quantitatively account for posttetanic potentiation (Delaney et al. 1989) and augmentation (Delaney and Tank 1994). Imaging analysis on the F1 and F2 components of facilitation has been less extensive because of the faster decay of their time course (Wu and Saggau 1994). Furthermore, it has been demonstrated that all four components of short-term enhancement can be interrupted by photolabile calcium buffer (Kamiya and Zucker 1994). Therefore all four components are driven by calcium, but the molecular mechanisms by which each component achieves its own kinetic and pharmacological properties remain unknown.

Over a period of several decades, the kinetic properties of synaptic facilitation have been analyzed to a high degree of precision (See Magleby 1987 for review). Typically, a burst of presynaptic action potentials is used to activate facilitation and a single action potential is then delivered at a defined delay to monitor facilitation (Magleby 1987; Mallart and Martin 1967). This experimental paradigm contains two separate components: activation and detection. To study the activation of facilitation, one varies the number and frequency of the conditioning action potentials (Balnave and Gage 1977; Bittner 1989; Linder 1974; Mallart and Martin 1967). Because of the stereotypical waveform of action potentials, it has not been possible to explore the detection aspect of facilitation. To investigate the activation and detection of facilitation, we have implemented a presynaptic voltage control method in the crayfish inhibitor (Vyshedskiy and Lin 1997), which exhibits robust facilitation under physiological conditions (Atwood and Bittner 1970; Dudel and Kuffler 1961). The use of controlled presynaptic pulses to investigate facilitation was first implemented in the squid giant synapse (Charlton et al. 1982). It was demonstrated

that presynaptic calcium current amplitude (I_{Ca}) did not increase during paired pulse facilitation. Perhaps because of the fact that the squid giant synapse is a phasic synapse that exhibits no synaptic enhancement under physiological conditions, there has been no further study of synaptic plasticity with controlled pulses in the latter preparation. In this report, we first demonstrate that the presynaptic voltage control method can be reliably used to analyze F2 facilitation at the inhibitor. The activation and detection of facilitation are then analyzed quantitatively. Results reported here provide quantitative information on synaptic facilitation that is impossible to obtain with the use of action-potential-based protocols.

METHODS

Animals and preparations

Crayfish (*Procambarus clarkii*) were obtained from Carolina Biological, Burlington, NC. Animals were maintained at 23°C until use. All experiments were performed at 15°C. The typical size of the animals was ~3.8 cm head to tail. The opener muscle of the first walking leg was used for all experiments. Details of the experimental setup have been described before (Vyshedskiy and Lin 1997). Briefly, a presynaptic voltage electrode always penetrated a secondary axon, whereas a presynaptic current electrode penetrated the main branch point of the inhibitor. The voltage electrode was routinely placed 100–150 μ m from the main branch point. Two postsynaptic electrodes penetrated a muscle fiber near the presynaptic voltage electrode. The electrode placements around the primary branch point limited our recordings to central muscle fibers. A GeneClamp 500 (Axon Instruments) was used for presynaptic voltage control, and two IE-201 intracellular amplifiers (Warner Instrument) were used to record from muscle fibers. Data were digitized with ITC-16 Mac interface (Instrutech). Pulse Control (J. Herrington and R. J. Bookman, University of Miami, Coral Gables, FL) was used for the control of data acquisition. Experimental data were typically filtered at 1.5–2 kHz and digitized at 10 kHz. All the data analysis was performed in Igor (Wavemetrics).

Dissection and the initial presynaptic electrode penetrations were conducted in a control saline [composition, in mM: 195 NaCl, 5.4 KCl, 13.5 CaCl₂, 2.6 MgCl₂, and 10 Na-*N*-2-hydroxyethylpiperazine-*N'*-2-ethanesulfonic acid (NaHEPES), pH 7.4]. After presynaptic electrode penetrations, the control saline was replaced by an experimental solution [composition: 155 mM NaCl, 40 mM tetraethylammonium chloride (TEACl), 5.4 mM KCl, 10 mM CaCl₂, 6.1 mM MgCl₂, 10 mM NaHEPES, 1 mM 4-aminopyridine, and 300 nM tetrodotoxin, pH 7.4]. The presynaptic voltage electrode contained 1 M CsCl, 0.6 M TEACl, and 0.6 M KCl and had a resistance of 20 M Ω . Presynaptic current electrodes had a resistance of 6–10 M Ω and contained 3 M KCl. Muscle electrodes contained 3 M KCl and had a resistance of 6–10 M Ω . All chemicals were purchased from Sigma unless otherwise indicated.

A common problem of the preparation was that a muscle fiber often received synaptic input from two or more branches whose electrotonic distance from the presynaptic voltage electrode varied. When it was possible to visualize the more distant one of the multiple branches in an unstained preparation, we tried to break the distant branch by pulling it with forceps. In general, it was possible to predict the presence of such distant branches from electrophysiological recordings (Vyshedskiy and Lin 1997). However, morphological examination of investigated terminal branches was performed after each experiment by sketching or photography. The inhibitor and excitor were stained with methylene blue (1 mM) for 7 min, or 4-(diethylaminostyryl)-*N*-methylpyridinium iodide (4-Di-2-Asp, 5 μ M; Molecular Probes) for 2 min, to verify

the origin and distribution of terminal branches on the muscle fiber studied.

Data analysis

CHLORIDE EQUILIBRIUM POTENTIAL. Although we were able to insert two microelectrodes into muscle fibers, postsynaptic voltage clamp was not used because simultaneous pre- and postsynaptic voltage clamp significantly increased the background noise level. However, current-clamp recording of the inhibitory postsynaptic potential (IPSP) does not always accurately reflect the quantity of transmitter release. The relationship between IPSP amplitude and transmitter release is not linear if the chloride driving force (ΔE_{Cl}) is small (Martin 1955). To correct for the resulting nonlinearity, chloride equilibrium potential (E_{Cl}) was measured in every experiment. ΔE_{Cl} , calculated as the difference between E_{Cl} and resting membrane potential, was measured after each experimental protocol and up to 20 measurements were made in some preparations. Typically, E_{Cl} reached a steady state 5–10 min after a muscle fiber was penetrated and E_{Cl} remained stable, with a drift of <5%, for \geq 4 h.

The nonlinear summation of IPSPs was corrected by the following equation

$$\text{IPSP}_{\text{COR}} = \frac{\text{IPSP}_{\text{peak}}}{1 - \frac{\text{IPSP}_{\text{peak}}}{\Delta E_{Cl}}}$$

where IPSP_{COR} represents corrected IPSP amplitudes and $\text{IPSP}_{\text{peak}}$ represents IPSP peak amplitude before correction. This equation is identical to the formulation by Martin (1955). The validity of this equation for the crayfish inhibitor synapse has been demonstrated in a previous study (Vyshedskiy and Lin 1997). ΔE_{Cl} recorded in each preparation is listed in corresponding figure legend.

In this report, corrected IPSP amplitudes are used for all of the plots, whereas recorded traces are displayed without correction. Therefore all of the quantitative analysis is discussed in terms of corrected peak IPSP amplitude, which is proportional to the total amount of transmitter release (Vyshedskiy and Lin 1997).

PRESYNAPTIC SPACE CLAMP. Because of the quantitative nature of this study, only those preparations whose presynaptic space constants are >8 times longer than their own lengths are used for further analysis. The presynaptic space constant is estimated on the basis of the shape of the depolarization-release (D-R) coupling plot of IPSPs triggered by calcium current activated during a 5-ms presynaptic pulse (IPSP_{ON}). The D-R coupling plot is then compared with that of the squid giant synapse, which is assumed to have an infinitely long space constant (Smith et al. 1985). If the data points from a given inhibitor fall within an envelope constructed from the D-R coupling curves of the squid giant synapse and a model presynaptic terminal with a space constant 8 times as long as its actual length, the inhibitor is considered to have a presynaptic space constant >8 times longer than its length. Figure 1 illustrates the D-R coupling plot of all the preparations used in this report; each preparation is plotted with the use of a separate symbol. Almost all of the data points are within the area enclosed by the two curves, and occasional deviations are due to noise. We did not routinely depolarize the inhibitor beyond +10 mV because further depolarization often damaged the axon. Furthermore, large presynaptic depolarizations introduce additional complications. For example, it was shown that total transmitter release is significantly affected by the facilitation process that occurs within the 5-ms presynaptic pulse during large presynaptic pulses (Augustine et al. 1985b). In addition, the relationship between presynaptic calcium current and postsynaptic response becomes complicated with large presynaptic pulses (Augustine and Charlton 1986). Given these considerations, results presented in

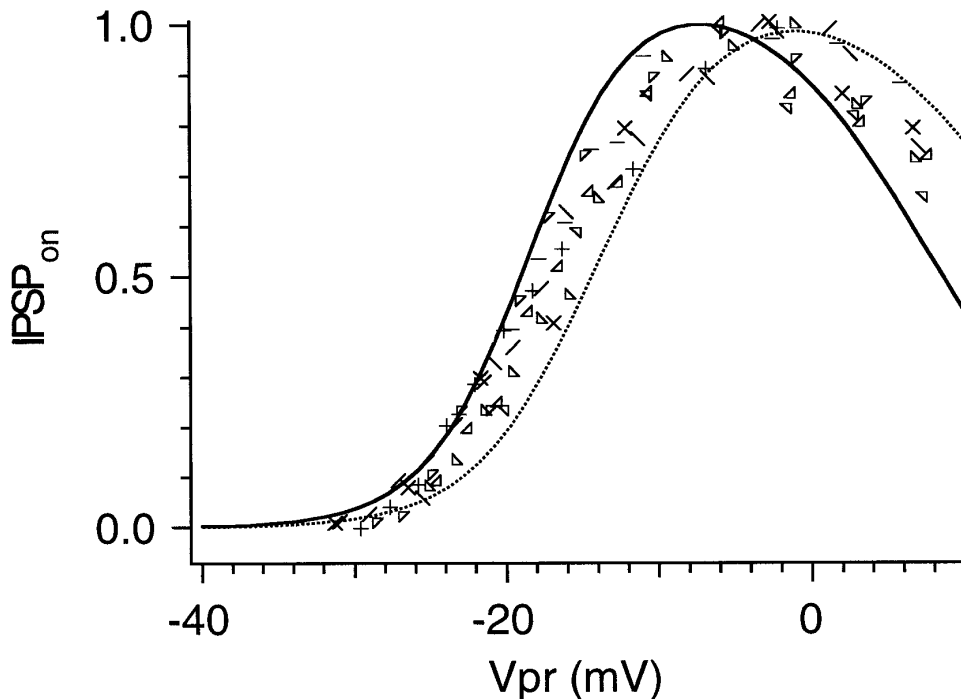


FIG. 1. Estimation of the presynaptic space constant of the inhibitor. Depolarization-release (D-R) coupling plots, measured from presynaptic pulse ($IPSP_{ON}$), of individual preparations are illustrated in different symbols ($n = 9$). $IPSP_{ON}$ was measured at 2.5 ms after the end of 5-ms pulses (Vyshedskiy and Lin 1997). Maximal level of release is normalized to 1 in all preparations. X-axis: level of presynaptic depolarization. To facilitate comparison of experimental data with theoretical curves, small variations in the X-axes of individual preparations are eliminated by shifting them horizontally by less than ± 3 mV. Similar alignment method was used for construction of other composite graphs in this paper. Solid curve: best fit of the D-R coupling plot of the squid giant synapse where the presynaptic spatial nonuniformity is minimized (Smith et al. 1985). Dotted curve is derived from a presynaptic model in which the release properties of the release sites are identical to those of the squid giant synapse but the axon has a space constant 8 times longer than its own length (Vyshedskiy and Lin 1997). A D-R coupling curve falling between the 2 curves is considered to be mediated by an inhibitor with a presynaptic space constant ≥ 8 times longer than its own length.

this study are limited to those mediated by presynaptic depolarization to < 0 mV.

MEASUREMENTS OF SYNAPTIC FACILITATION. Facilitation is measured by comparing the peak amplitude of a control IPSP ($IPSP_{cnt}$) with that of a test IPSP ($IPSP_{test}$). Both IPSPs are activated by the same test pulse but, only $IPSP_{test}$ is facilitated by a preceding conditioning stimulation. Facilitation is quantitated by two parameters: normalized facilitation (F_n) and absolute facilitation (F_a). F_n follows the traditional method for normalizing facilitation, $F_n = (IPSP_{test} - IPSP_{cnt}) / IPSP_{cnt}$, whereas F_a is equal to the difference between $IPSP_{test}$ and $IPSP_{cnt}$ ($F_a = IPSP_{test} - IPSP_{cnt}$). In the protocols in which a test pulse of constant amplitude is used, such as when the decay of facilitation is monitored, F_n and F_a provide the same information and are related to each other by a constant scaling factor, $IPSP_{cnt}$. However, when the amplitude of test pulse is changed systematically, F_n and F_a may exhibit different dependence on test pulse amplitude. Under these conditions, the presentation of both parameters provides a more complete description of the facilitation process.

SELECTION OF 5-MS PRESYNAPTIC PULSES. We used 5-ms presynaptic pulses to perform all of our experiments for the sake of optimizing signal-to-noise ratio (Vyshedskiy and Lin 1997). Action-potential-like 2-ms pulses trigger small IPSPs (50–120 μ V), which require an unrealistically large number of repeats to achieve an acceptable averaged trace. As a result, 2-ms pulses provide a narrow range of measurable IPSP amplitudes, ~ 2 – 3 -fold change for the entire range of the D-R coupling plot tested (unpublished observations). In contrast, IPSP amplitudes activated by 5-ms pulses vary ≥ 10 -fold over the same range of the D-R coupling plot tested. The large transmitter release activated by 5-ms pulses is assumed not to saturate the transmitter release machinery according to two criteria. First, 5-ms pulses are capable of triggering a higher level of release at physiological levels of extracellular free calcium ions ($[Ca^{2+}]_o$; 13.5 mM), which is higher than the 10 mM concentration used in this study. Second, a 20-ms presynaptic pulse is able to activate an IPSP that is 5–10 times larger than that activated by a 5-ms pulse of the same amplitude (Vyshedskiy

and Lin 1997). Therefore presynaptic pulses with a duration of 5 ms are a reasonable choice for the present study.

RESULTS

Facilitation activated by presynaptic voltage controlled-pulses

An example of facilitation activated by controlled presynaptic pulses is illustrated in Fig. 2. Pairs of 5-ms presynaptic pulses of identical amplitude are superimposed (*bottom traces*). The second 5-ms pulse of each pair activates a significantly larger IPSP (*top traces*). The enhanced transmitter release shown here mainly reflects the F2 component of facilitation, because the interpulse interval is ~ 150 ms.

Similar to the excitor (Bittner 1989), the inhibitor of the crayfish opener muscle exhibits both the F1 and F2 components of facilitation. Figure 3 illustrates an example of the two components in an inhibitor where facilitation is activated by a burst of five action potentials (Fig. 3A, \). Figure 3A shows superimposed traces where facilitation is monitored at different delays following the conditioning stimulation. The decay time course of facilitation is plotted in Fig. 3B, where the F1 and F2 components exhibit decay time constants of 13 and 500 ms, respectively. In six preparations in which the F1 component was monitored, it decayed with a time constant of 18.9 ± 4.1 (SD) ms. The F2 component exhibits an averaged decay time constant of 521 ± 107 ms ($n = 11$). Therefore the F1 component should have decayed to a near-zero level at 150 ms following a conditioning stimulation, and the facilitation detected at this delay reflects mainly the F2 component of facilitation.

To verify that facilitation activated by 5-ms presynaptic pulses corresponds to the F2 component activated by action potentials, the decay time course of facilitation activated by

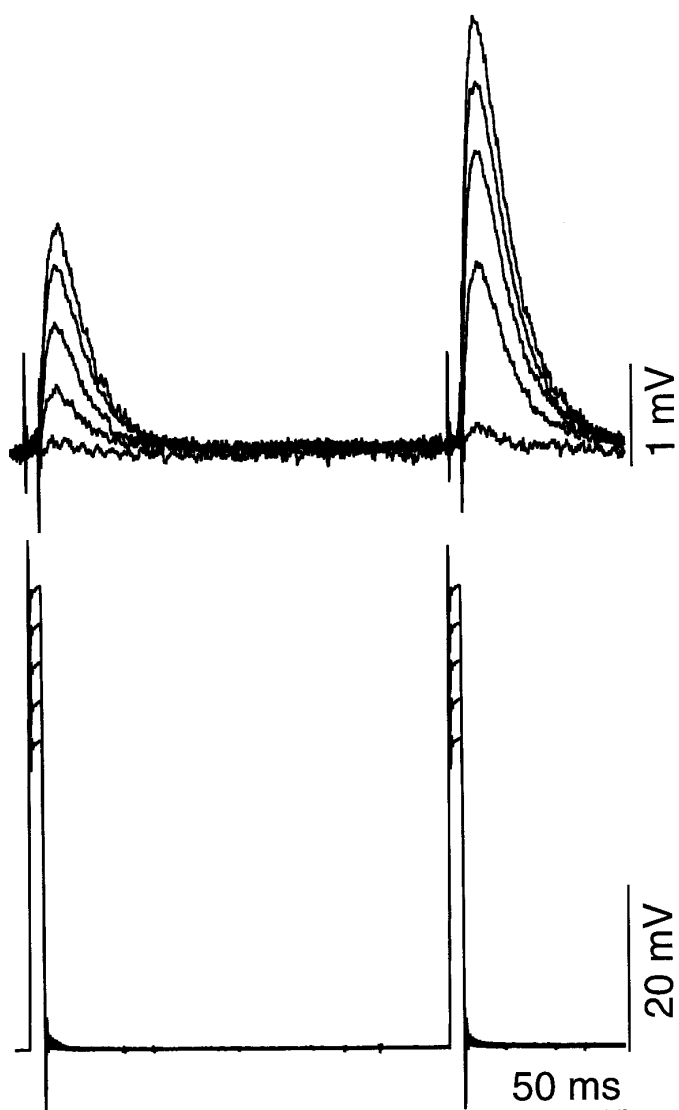


FIG. 2. Demonstration of facilitation activated by paired presynaptic pulses. Paired pulses of identical amplitudes in the inhibitor (*bottom traces*) are able to activate synaptic facilitation. Presynaptic pulses have a duration of 5 ms and are separated by an interval of 150 ms. The 2nd inhibitory postsynaptic potential (IPSP) of each pair exhibits a larger amplitude (*top traces*). Holding potential of the inhibitor: -75 mV.

5-ms pulses was measured. Figure 4A shows an example in which a single 5-ms pulse is used to trigger a constant facilitation while a second 5-ms test pulse is delivered at different intervals to monitor the decay of facilitation. The decay time constant of facilitation is 685 ms (Fig. 4B). Figure 4C illustrates an averaged decay time course of facilitation activated by a single 5-ms pulse, with a time constant of 880 ms ($n = 12$). Although this decay time constant is larger than that activated by action potentials, it is still well within the range of F2 facilitation. The difference could be due to a slight contaminating augmentation component activated by 5-ms pulses. All the experimental protocols were repeated at a rate of 0.2 Hz to ensure that facilitation had decayed to zero between trials.

To quantitatively analyze synaptic facilitation with the presynaptic voltage control method, we must first establish

that the quality of presynaptic voltage control during the time window of F2 facilitation is not changed by the conditioning stimulations. This issue was addressed by experiments shown in Fig. 5. Figure 5A, *top traces*, demonstrates a clear facilitation activated by a conditioning pulse. Figure 5A, *bottom traces*, shows the corresponding presynaptic recordings in which the effects of the conditioning pulse on the amplitude of the test pulse are compared. The preceding conditioning pulse decreases the test pulse amplitude slightly. These effects are only detectable under high amplification (Fig. 5A, *inset*). The difference in amplitude at the end of the 5-ms test pulse is 0.18 mV ($\text{Diff } V_{\text{test}}$). Figure

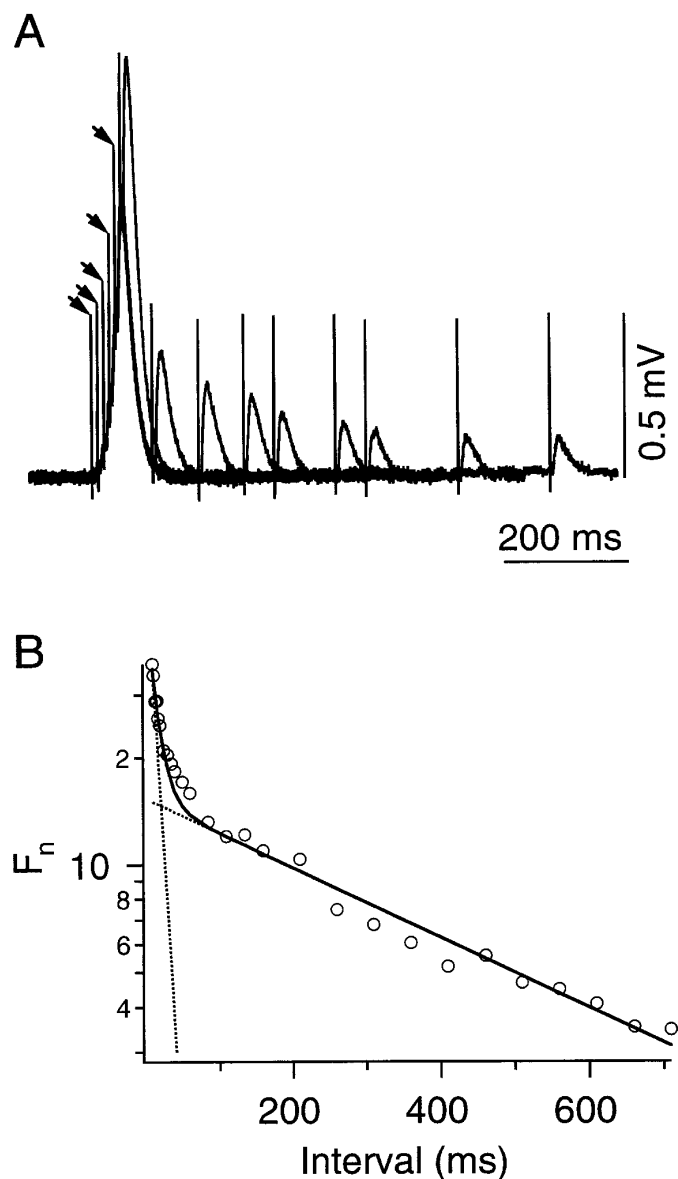


FIG. 3. Multiple components of synaptic facilitation at the inhibitor of the crayfish opener muscle. *A*: superimposed traces showing the decay of facilitation after a conditioning stimulation of 5 action potentials (\setminus). *B*: decay of synaptic facilitation can be separated into 2 components with time constants of 13 and 500 ms, respectively. Dotted lines: best exponential fits of the 2 components. This experiment was performed in control solution. Amplitude of control IPSP: 22.3 μV . Chloride driving force (ΔE_{Cl}) = 13 mV. This experiment was performed in physiological saline.

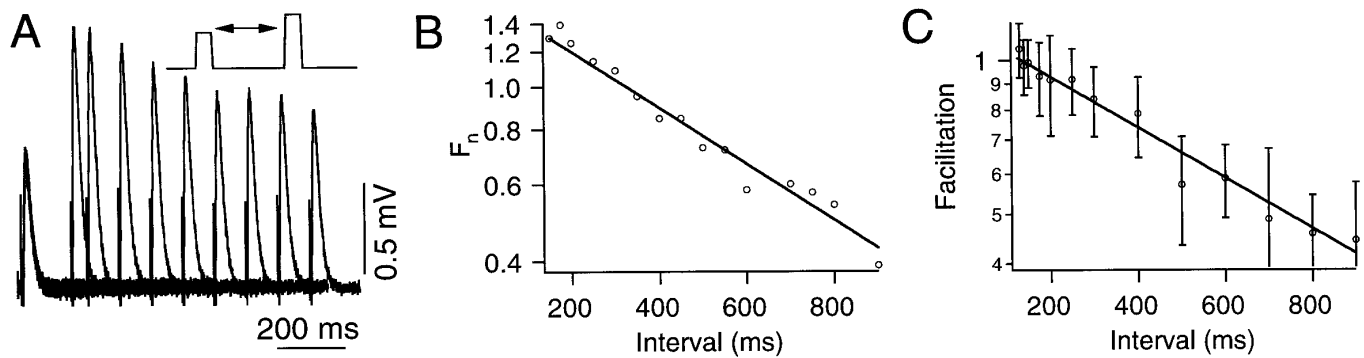


FIG. 4. Decay time course of synaptic facilitation activated by presynaptic voltage-controlled pulses. *A*: superimposed traces illustrating the decay of facilitation following a single 5-ms conditioning pulse. *B*: decay time constant measure from the recordings shown in *A* is 612 ms. $\Delta E_{Cl} = 6.5$ mV. *C*: averaged results of the decay of facilitation measured from 12 preparations. Normalized facilitation (F_n) in each preparation was calculated 1st. The values of F_n measured at 135, 150, and 175 ms were then averaged and the average was used to normalize the magnitude of facilitation. Data displayed here are the average of normalized data from 12 preparations.

5*B* shows a typical experiment in which the impact of conditioning pulse amplitudes on the amplitude of a test pulse is analyzed systematically. The difference is normalized by the

amplitude of the control test pulse, i.e., the test pulse that is not preceded by a conditioning pulse, and is always <1%. For example, when the conditioning pulse was depolarized

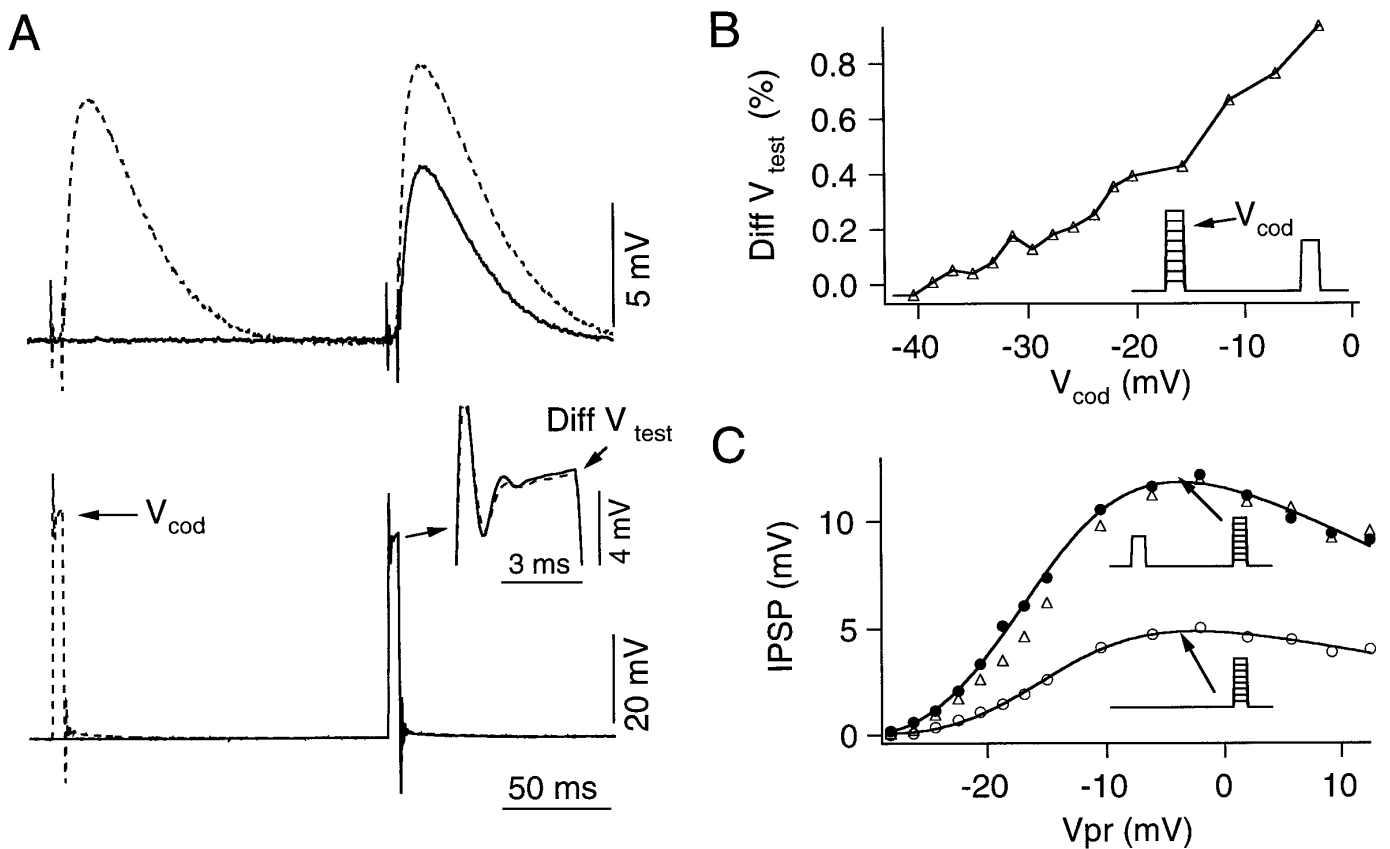


FIG. 5. Control of presynaptic potential during facilitation. *A*: example of facilitation activated by a single 5-ms conditioning pulse. Solid traces: control pre- and postsynaptic recordings. Dashed traces: test recordings. *Inset*: peaks of test pulses, with and without conditioning pulses, displayed at a high magnification. Presynaptic holding potential: -70 mV. *B*: effect of conditioning pulse amplitude (V_{cod}) on amplitude of the test pulse. *X*-axis: level of presynaptic depolarization, measured by averaging the potential between the 3rd and 5th ms of the pulses. *Y*-axis: change of presynaptic test pulse amplitude caused by the conditioning pulse. Plot is taken from the experiment shown in *A*. Difference is normalized by control pulse amplitude (47 mV). *C*: conditioning pulse has a minimal effect on D-R coupling. A control D-R coupling curve (\circ) is similar to that of the facilitated IPSP (\bullet) in 2 respects: they have the same threshold and the suppression of release starts at the same point. Δ , control IPSPs scaled to the height of the facilitated IPSPs. *Inset*: protocol used to obtain each plot. Data were obtained from the same synapse as shown in *A*. $\Delta E_{Cl} = 16$ mV. V_{pr} , level of presynaptic depolarization.

to -11 mV from a holding potential of -70 mV, it caused the peak level of the test pulse to deviate by 0.7%. In eight preparations, conditioning pulses depolarized to between -10 to 0 mV caused a deviation of 0.4–0.9% in test pulse amplitudes. Therefore the presence of the conditioning pulse does not lead to a significant difference in the amplitude of the test pulse during the time window of F2 facilitation. Although the small deviation demonstrated in Fig. 5, *A* and *B*, is reassuring, this observation by itself does not provide information on the quality of space clamp along the presynaptic axon.

The quality of space clamp can be evaluated by comparing the D-R coupling curves of control and facilitated IPSPs. Figure 5*C* shows that the D-R coupling plots for control (\circ) and facilitated (\bullet) IPSPs have the same threshold and maximum, as indicated by the comparison between the facilitated IPSPs with the control IPSP scaled to the same height (Δ). (The difference on the rising phase between the facilitated and scaled control IPSPs has to do with a reduction of calcium cooperativity of transmitter secretion during facilitation; see below). Because the threshold of release and the maximal point are reliable indicators for the quality of presynaptic space clamp (Vyshedskiy and Lin 1997), the similarity between the two plots would suggest that the presynaptic space constant is not significantly changed during facilitation.

To ensure that the presynaptic voltage control method does not compromise the viability of the release and facilitation mechanisms, we compared the magnitude of facilitation activated by presynaptic pulses with that activated by action potentials. Figure 6 shows an example in which the facilitation is activated by a 5-ms conditioning pulse and monitored by a 2-ms pulse, which approximates the waveforms of action potentials at 15°C . The presence of conditioning stimulation triggers a clear increase in $\text{IPSP}_{\text{test}}$ amplitude (---). In 10 preparations in which 2-ms pulses depolarized to 0 mV were used to monitor facilitation activated by a 5-ms pulse, the average magnitude of F_n is 5.72 ± 1.69 . Average F_n activated by a burst of 10 action potentials is 6.17 ± 1.68 ($n = 27$). Therefore facilitation activated by presynaptic voltage-controlled pulses is comparable in magnitude with that activated by action potentials. Finally, the stability of the facilitation process is not affected by the presynaptic voltage control method. The magnitude and decay time constant of facilitation remain unchanged for up to 6 h in most preparations.

Activation of facilitation

Given the large degree of freedom in the control of the amplitude and duration of presynaptic pulses, we first determined the impact of 5-ms conditioning pulse amplitudes on the magnitude of facilitation. This goal was achieved with the use of an activation protocol in which the amplitude of a conditioning pulse was changed systematically while the magnitude of facilitation is monitored by a test pulse of constant amplitude (see Fig. 5*B*, *inset*, for an illustration of the activation protocol). Two examples of recordings are superimposed in Fig. 7*A*. The small conditioning pulse, which does not trigger any transmitter release on its own, has already activated detectable facilitation (—). The

larger conditioning pulse, which triggers a detectable conditioning IPSP (IPSP_{cod}), activates a higher level of facilitation (---).

Figure 7*B* illustrates the dependence of F_a (Δ) on the level of depolarization of conditioning pulses (activation curve). For the purpose of comparison, the D-R coupling plot of the conditioning pulses is also illustrated (\circ). A significant level of facilitation has already been activated before the conditioning pulse itself triggers any release (arrow labeled 1). Furthermore, the maximal level of facilitation is achieved before the D-R coupling curve of IPSP_{cod} s reaches its maximal level (arrow labeled 2). These characteristics are consistent findings. Figure 8*A* shows average results obtained from eight preparations, in which a significant level of facilitation is observed before IPSP_{cod} is detectable (arrow labeled 1) and F_a reaches its plateau level before IPSP_{cod} reaches its maximum (arrow labeled 2).

The different shapes of the activation curve and the D-R coupling curve of the IPSP_{cod} suggest that the activation of facilitation and the transmitter secretion processes may have different calcium cooperativities. We next tried to compare the calcium cooperativity of the activation process with that of the secretion step by assuming that the calcium influx that activated IPSP_{cod} was related to the IPSP_{cod} amplitude by a fixed power relationship. Under this assumption, a double logarithm plot of the magnitude of facilitation, represented by F_a , against IPSP_{cod} should provide a comparison of the calcium cooperativity of the two processes. A slope of 1 implies that the calcium cooperativity of activating facilita-

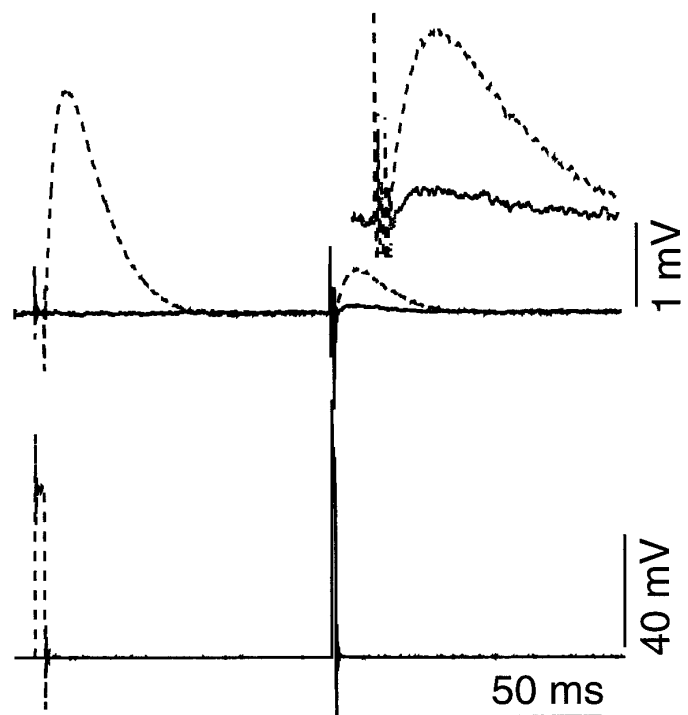


FIG. 6. Presynaptically controlled pulses activate synaptic facilitation with a magnitude similar to that activated by action potentials. A 5-ms conditioning pulse was used to trigger facilitation, whereas a 2-ms test pulse was used to monitor the magnitude of facilitation. Control IPSP (IPSP_{cnt} ; —) was recorded in the absence of a preceding conditioning pulse. Test IPSP ($\text{IPSP}_{\text{test}}$; ---) was facilitated by the preceding pulse. *Inset*: IPSP_{cnt} and $\text{IPSP}_{\text{test}}$ a higher amplification.

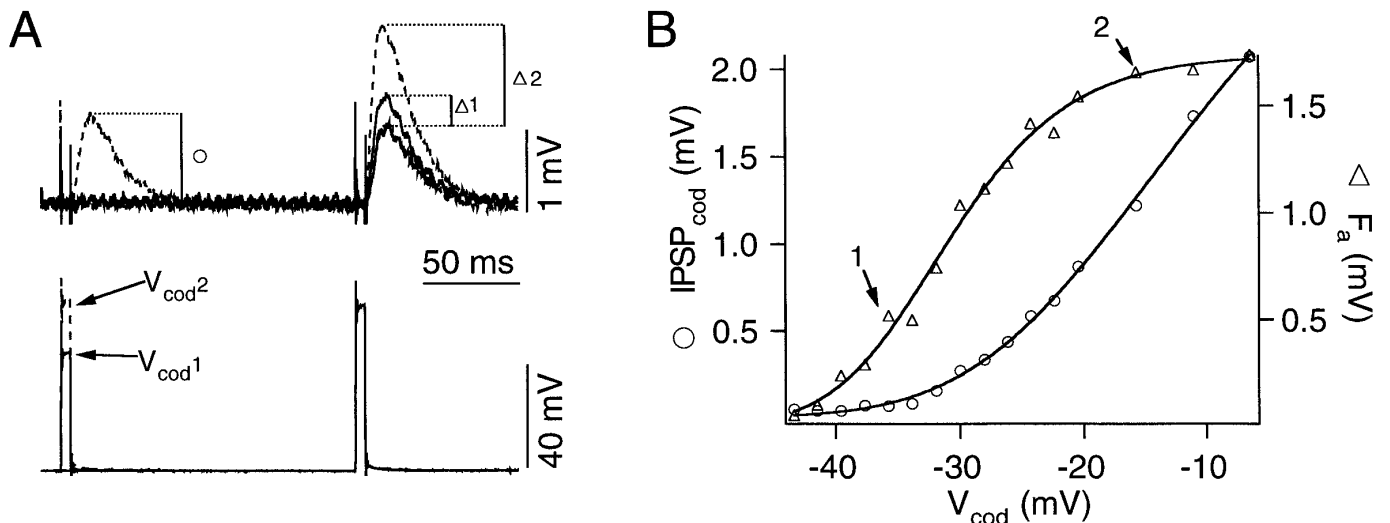


FIG. 7. Analysis of the activation protocol. *A*: examples of recordings obtained from the activation protocol. Two levels of conditioning pulses are illustrated. The small conditioning pulse (—) does not activate any IPSP by itself but has triggered a low level of facilitation. The large conditioning pulse (---) activates a detectable IPSP and triggers a higher level of facilitation. *B*: comparison of D-R coupling curve of the conditioning pulse with the magnitude of facilitation activated by the conditioning pulse. Facilitation appears before the conditioning pulse is able to activate detectable release (arrow labeled 1). Magnitude of facilitation saturates at a level at which the conditioning pulse reaches 55% of its maximal release (arrow labeled 2). Arrows also identify data points corresponding to traces in *A*. $\Delta E_{Cl} = 10.6$ mV. $IPSP_{cod}$, conditioning IPSP.

tion is the same as that of the secretion processes. The double logarithm plot of the averaged data shown in Fig. 8*B* gives rise to a slope of 0.34. (The slopes measured from individual experiments varied from 0.27 to 0.43, 0.34 ± 0.06 , $n = 8$.) The slope suggests that the activation process of facilitation has a lower calcium cooperativity than that of the secretion process.

The plateau phase of the activation curve could be due to saturation of the facilitation process or it could be due to the possibility that the test pulse may not be able to detect the full extent of facilitation. The second possibility was tested by repeating the activation protocol with test pulses

of different amplitudes. Figure 9*A* shows two recordings in which $IPSP_{cod}$ amplitudes are identical but the facilitation is monitored by two different test pulses. The solid and dotted traces represent facilitation monitored by a small and large test pulse, respectively. Figure 9*B* illustrates the comparison between the activation curves obtained from the small (open squares) and large (open circles) test pulses. The similarity between the two curves is highlighted by scaling the activation curve mediated by small test pulses to the same height as that mediated by large pulses (filled circles connected by dotted lines). The levels of presynaptic depolarization at which the F_a curves reach their saturation are similar. There-

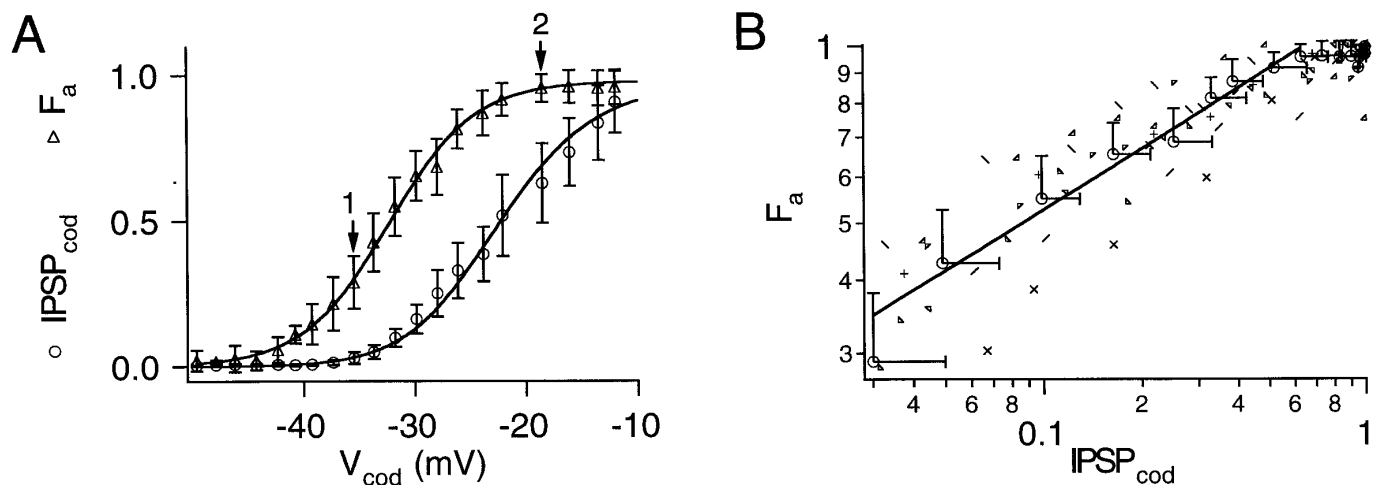


FIG. 8. Averaged results obtained from the activation protocol. *A*: averaged activation curve obtained from 8 preparations (Δ) and average of the corresponding D-R coupling curves of $IPSP_{cod}$. Maxima of both parameters were scaled to 1 before data averaging from the different preparations was performed. Arrows: range of data used in linear fit of double logarithm plot in *B*. *B*: normalized absolute facilitation (F_a) plotted against normalized $IPSP_{cod}$ on double logarithmic scales; slope is 0.34. Normalized data obtained from individual experiments are also shown with different symbols. Because a test pulse of constant amplitude is used in this protocol, F_a and F_n provide the same slope on the double logarithm plot.

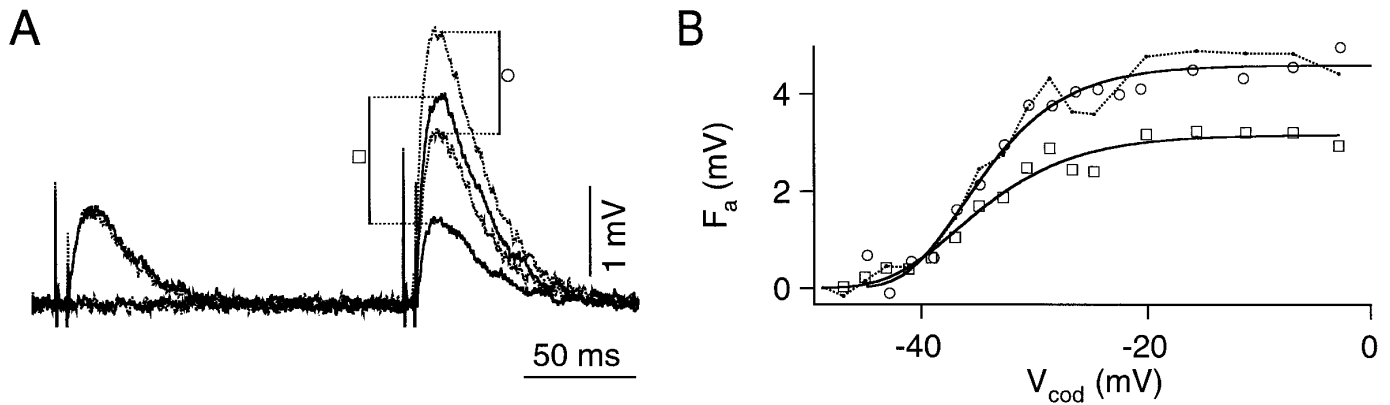


FIG. 9. Saturation of activated facilitation is not an artifact of the detection process. *A*: examples of recordings in which facilitations activated by the same conditioning stimulation, as indicated by the same $IPSP_{cod}$ amplitude, were monitored by 2 test pulses. Facilitation detected by a small test pulse is shown in solid traces and highlighted by open squares. Facilitation detected by a large test pulse is shown in dotted traces and highlighted by open circles. The $IPSP_{cod}$ activated by the large test pulse is roughly twice as large as that activated by the small test pulse. *B*: comparison of the activation curves as tested by small (open squares) and large (open circles) test pulses. The 2 curves are identical to each other. Filled circles connected by dotted lines: data scaled from the activation curve of the small test pulse. Amplitude of F_a is significantly larger than that shown in the traces in *A* because the nonlinear summation of IPSP has been compensated. $\Delta E_{Cl} = 5.8$ mV.

fore the plateau phase of the activation curve is not an artifact associated with test pulse amplitude and it should represent a saturation of the facilitation process.

Activation of facilitation with subthreshold conditioning pulses

We utilize two main observations of the activation process observed thus far to design a protocol that enables us to study synaptic facilitation in the absence of any possible transmitter depletion. First, a conditioning pulse that is subthreshold to transmitter release is able to activate a significant level of facilitation. Second, a conditioning pulse that is 15 mV above release threshold is able to reach the plateau region of the activation curve and activate a maximal facilitation. With the use of these two findings, we next demonstrate that a burst of eight subthreshold conditioning pulses, although not triggering any release itself, activates a near-maximal facilitation. An example of facilitation activated by eight subthreshold conditioning pulses is illustrated in Fig. 10A. The conditioning pulses do not trigger any detectable IPSP. The upward-going spikes are artifacts. Two levels of test pulses are illustrated; the results obtained from the small test pulse are shown with solid traces, whereas those from the large test pulse are shown with dashed traces. The D-R coupling plots of the test pulses with (●) and without (○) conditioning stimulation are shown in Fig. 10C. (Increasing the number of subthreshold conditioning pulses did not further increase the magnitude of facilitation; data not shown.) Examples of recordings of facilitation activated by a single and suprathreshold conditioning pulse from the same synapse are illustrated in Fig. 10B, and its D-R coupling curves are plotted in Fig. 10C (□, ■). The two types of conditioning stimulations activate comparable levels of facilitation. The normalized difference of maximal F_a activated by one suprathreshold conditioning pulse versus eight subthreshold conditioning pulses was averaged from eight preparations. (The normalization was achieved by dividing the difference of maximal F_a s by the maximal F_a activated by 8 subthresh-

old conditioning pulses.) The average is statistically not different from zero (0.01 ± 0.23). Therefore eight subthreshold conditioning pulses are able to trigger a maximal level of facilitation without any detectable transmitter release.

Finally, to ensure that facilitation activated by eight subthreshold conditioning pulses does not activate additional components of short-term plasticity, we also examined the decay time constant of facilitation activated by eight subthreshold pulses. Figure 11A illustrates examples of recordings obtained from such a protocol in which facilitation is monitored at 200, 500, and 800 ms after the end of the conditioning stimulation. The decay time constant measured from this example is 737 ms (Fig. 11B). Decay of facilitation activated by eight subthreshold pulses and averaged from six preparations is shown in Fig. 11C (open circles), and the time constant was 957 ms. The decay time constant is identical to those activated by single suprathreshold pulses (filled circles), because the SD bars calculated from the two protocols overlap considerably. Therefore repetitive application of subthreshold conditioning pulses is able to activate the F2 component of facilitation to its maximal level without triggering any conditioning release.

Detection of facilitation

The two experimental protocols shown in Fig. 10 were used to compare the magnitudes of facilitation activated by two types of conditioning stimulation. The same protocols were also used to examine the detection of facilitation. Specifically, these protocols use a constant conditioning stimulation to activate a fixed level of facilitation and change test pulse amplitude systematically to determine whether test pulses of different amplitudes can detect the same level of facilitation. The D-R coupling plots for control and facilitated release shown in Fig. 10C can be replotted to illustrate the dependence of F_a (Δ) and F_n (○) on the level of depolarization of test pulses (Fig. 12A). Typically, F_a increases as test pulse amplitude increases, whereas F_n is highest for the smallest test pulses. In other words, smaller test pulses are able to detect a proportionally

higher level of facilitation, whereas larger test pulses are better able to reveal the "full extent" of facilitation. This is a consistent finding. Averaged and composite plots of F_n and F_a , from nine preparations, are illustrated in Fig. 12, *B* and *C*, respectively. In each case, open circles represent averaged data, whereas results obtained from individual experiments are shown in different symbols.

Taking an approach similar to the analysis of the activation process, we next examined the calcium cooperativity of transmitter release during facilitation. This was achieved by plotting $\text{IPSP}_{\text{test}}$ against IPSP_{cnt} on a double logarithm scale. Figure 12*D* illustrates the double logarithm plots of normalized data from nine preparations. The open circles represent the averaged data, and the best linear fit exhibits a slope of 0.77. (The slopes measured from individual experiments varied from 0.6 to 0.78, 0.73 ± 0.07 , $n = 9$.) Therefore there appears to be a decrease in calcium cooperativity of the secretion process during facilitation.

DISCUSSION

In this report we have demonstrated that the presynaptic voltage control method can be used to investigate the F2 component of synaptic facilitation. Two separate aspects of synaptic facilitation were examined: activation and detection. We found that the calcium cooperativity of the activation process is lower than that of the secretion process. In addition, we have demonstrated that it is possible to activate a high level of facilitation with conditioning pulses that are subthreshold to release. Results obtained from the detection protocol suggest that the calcium cooperativity of transmitter secretion is decreased during a maximal level of facilitation.

Five-millisecond presynaptic pulses consistently activate the F2 component of facilitation

This report mainly focuses on quantitative analyses of the F2 component of facilitation. We did not pursue the F1 component

because the amplitude difference between control and test presynaptic pulses was significant during the first 20 ms following a conditioning pulse (data not shown). This difference could be attributed to a strong calcium-activated potassium current activated by conditioning pulses (Sivaramakrishnan et al. 1991a). Therefore although 5-ms presynaptic pulses are capable of activating the F1 component of facilitation, the uncertainties of presynaptic voltage control during the F1 period prevented us from investigating F1 quantitatively.

Unlike with action-potential-based protocols, one cannot simply assume that the presynaptic pulses applied during facilitation depolarize release sites to the same level as those applied during control conditions. Two lines of independent evidence suggest that the quality of presynaptic voltage control during the time window of F2 facilitation is minimally affected by conditioning stimulation. First, the difference in the amplitude of control and test presynaptic pulses was insignificant; the maximal deviation is <1% of the control pulse amplitudes. Second, we have previously demonstrated that the shape of the D-R coupling curves is closely related to the presynaptic space constant (Vyshedskiy and Lin 1997). Identical threshold and maximum of control and facilitated D-R coupling curves reported here suggested that there is no detectable change in the presynaptic space constant during the time window of F2 facilitation (Fig. 5*C*). Finally, we have previously shown that IPSP amplitudes activated by 2-ms presynaptic pulses, which approximate the waveform of action potentials at 15°C, are similar to those activated by action potentials. We now further demonstrate in this report that the magnitude of facilitation tested by 2-ms pulses is comparable with that activated by a burst of five action potentials. Although a quantitative comparison of the magnitude of facilitation between the two experimental conditions is difficult to establish, the similar magnitudes of facilitation suggest that our preparation and experimental setup do not compromise the function of the synapse.

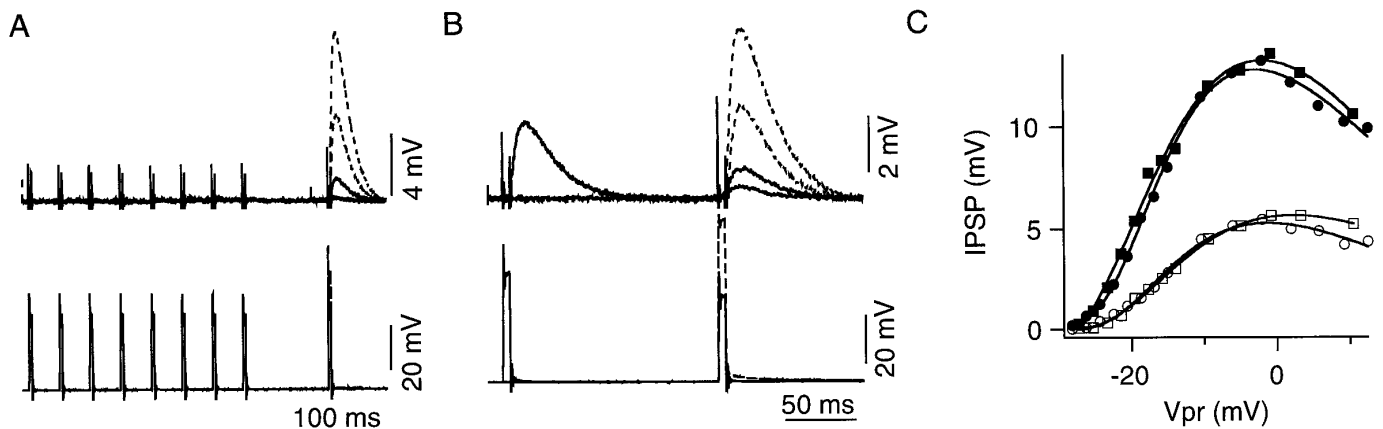


FIG. 10. It is possible to activate near-maximal facilitation with subthreshold conditioning pulses. *A*: examples of recordings in which 8 subthreshold conditioning pulses are used to activate facilitation. The conditioning pulses, each with a duration of 5 ms and delivered at 20 Hz, themselves do not trigger any release. Two levels of test pulses are illustrated. Solid traces: responses activated by the lower-level test pulse. Dashed traces: responses mediated by the upper-level test pulse. *B*: example of recordings in which facilitation is activated by a single suprathereshold conditioning pulse and monitored by 2 levels of test pulses. Solid traces: responses mediated by the lower-level test pulse. Dashed traces: traces associated with the upper-level test pulse. *C*: 2 types of conditioning stimulations activate a comparable level of facilitation. \circ , \bullet : D-R coupling plots of control and facilitated release, respectively, activated by 8 subthreshold conditioning pulses. \square , \blacksquare : D-R coupling plots of control and facilitated release activated by 1 suprathereshold conditioning pulse, illustrated for comparison. Results shown in this figure are obtained from the same preparation shown in Fig. 5*C*.

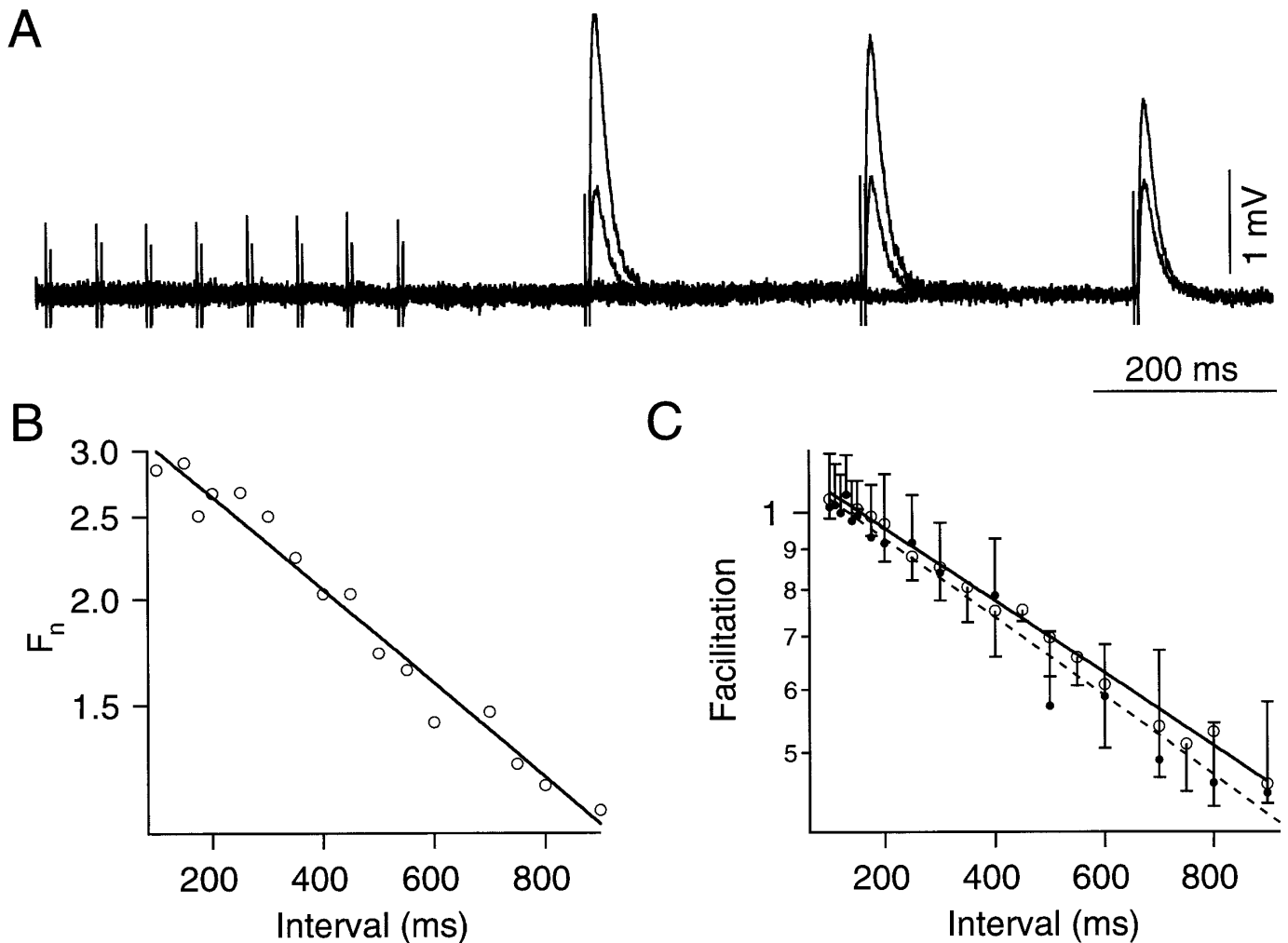


FIG. 11. Eight subthreshold conditioning pulses activate mainly the F2 component of facilitation. *A*: superimposed traces illustrating the decay of facilitation activated by 8 subthreshold conditioning pulses. Test pulses are delivered at 200, 500, and 800 ms after the conditioning stimulation. *B*: decay of facilitation measured from preparation shown in *A*. Best fit of the decay time constant is 737 ms. *C*: averaged results of the decay of facilitation activated by 8 subthreshold conditioning pulses (open circles). Decay time constant of the averaged result is 957 ms (—). Magnitudes of F_n at 135, 150, and 175 ms were 1st averaged in individual preparations, and the average was then used to normalize the magnitudes of facilitation. Normalized results from 6 preparations were then averaged. Filled circles and dashed line: decay, and its best fit, of facilitation activated by a single conditioning pulse (see also Fig. 4C). SD bars associated with open circles point downward, whereas those of filled circles point upward.

Presynaptic space clamp

All of the preparations used in this report were selected for their quality of presynaptic space clamp according to the characteristics of their D-R coupling curves. The uniformity of presynaptic space clamp in our preparation is also supported by the comparison between the facilitation activated by eight subthreshold conditioning pulses and that activated by one suprathreshold pulse (Fig. 10). Specifically, if there is a severe spatial anisopotentiality in the inhibitor, the subthreshold conditioning pulses must only facilitate proximal release sites. As a result, a single and suprathreshold conditioning pulses must be able to facilitate more release sites than subthreshold pulses and therefore must be able to activate a greater degree of facilitation. Because the magnitudes of facilitation activated by the two types of conditioning stimulation are identical, this would suggest that the spatial control of presynaptic potential is uniform.

Inspection of the activation protocol also suggests an adequate presynaptic space clamp. The magnitude of facilitation reaches a plateau level before conditioning pulses achieve a maximal level of release. If the higher level of facilitation activated by increasing amplitudes of conditioning pulse is caused by the recruitment of increasing numbers of release sites, as one would expect with a short presynaptic space constant, the magnitude of facilitation should continue to increase as long as $IPSP_{cod}$ s are increasing. Furthermore, we have also demonstrated that the shape of the activation curve is independent of test pulse amplitude. With poor presynaptic voltage control, one would expect that the activation curve monitored by large test pulses should reach its plateau at a more depolarized level, because a large test pulse would have been able to reveal facilitation over a longer stretch of presynaptic axon that could only be reached and facilitated by large conditioning pulses. In addition to the fact that the prepa-

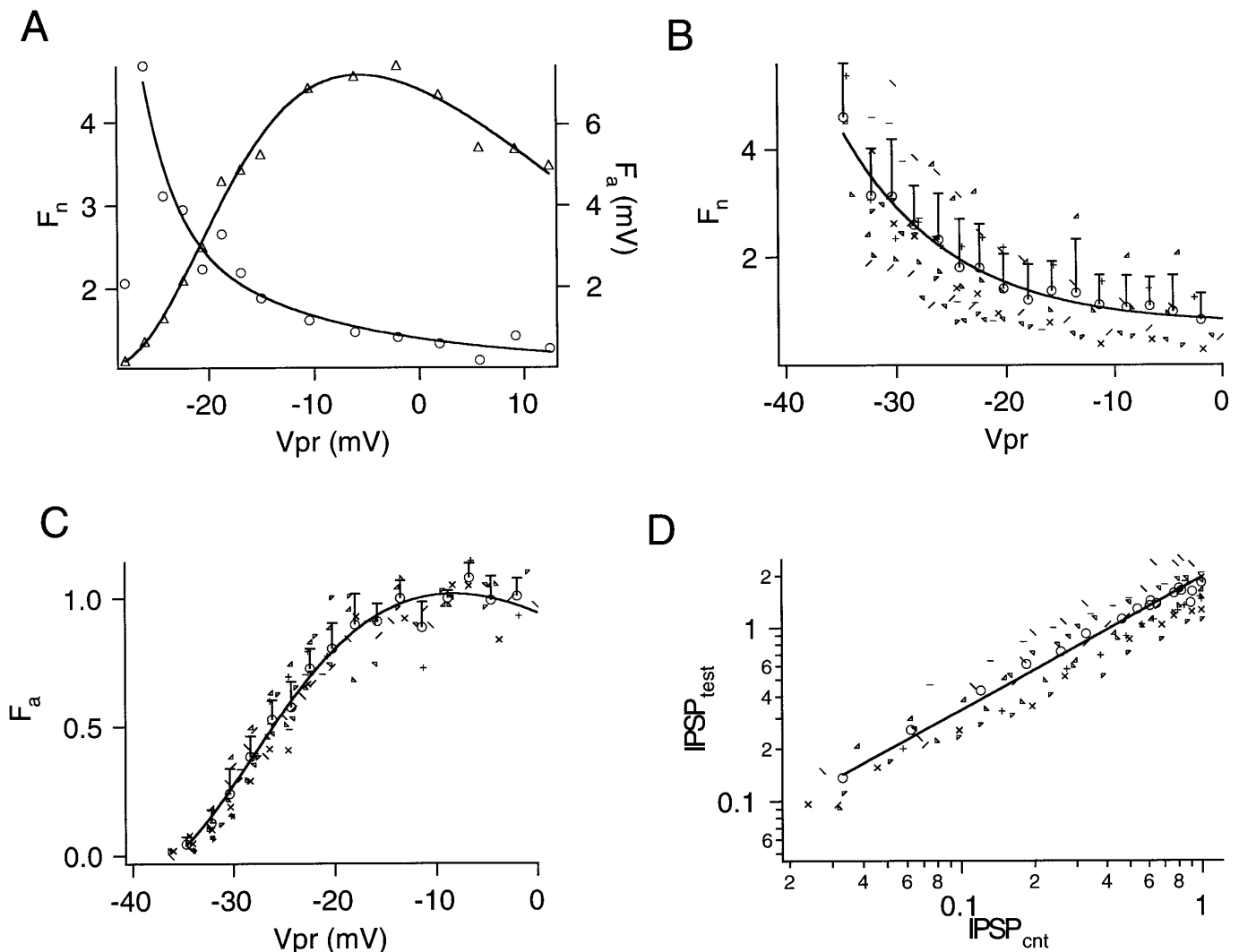


FIG. 12. Analysis of the detection process of facilitation. *A*: voltage dependence of F_a and F_n . X-axis: level of presynaptic depolarization of test pulses. Data are taken from the same preparation shown in Fig. 10. Because the 8 subthreshold and 1 suprathreshold conditioning pulses give rise to identical results, F_a and F_n shown in this graph have been averaged from data obtained with the use of both protocols. *B*: averaged and composite plot of F_n against presynaptic depolarization of the test pulse. Open circles: averaged results, with SD. Results from individual experiments are illustrated with the use of different symbols. The large SDs are due to variations in the magnitude of facilitation among preparations. The downward trend is a consistent observation among all of the individual preparations. Results illustrated here only include data points where IPSP_{cnt} amplitudes are significantly larger than background noise, i.e., $\text{IPSP}_{\text{cnt}} > 0.2$ mV. *C*: averaged and composite plot of F_a against presynaptic depolarization of the test pulses. The maximal level of F_a is normalized to 1 before the results from individual experiments are averaged. Mean (open circles) and SD are shown. Results from individual preparations are also illustrated with the use of different symbols. *D*: normalized $\text{IPSP}_{\text{test}}$ plotted against normalized IPSP_{cnt} on double logarithmic scales. Individual experiments are shown with different symbols, whereas averaged results are shown with open circles. IPSP_{cnt} and $\text{IPSP}_{\text{test}}$ are normalized by the maximal amplitudes of IPSP_{cnt} . A slope of 0.77 is obtained from the averaged data. The last 2 points of the data are not used in the curve fitting.

rations used in this report had been selected for their long presynaptic space constants, results obtained from activation and detection protocols provide further support for our previous conclusion that presynaptic space clamp of the inhibitor is uniform under our experimental conditions (Vyshedskiy and Lin 1997). In conclusion, results presented in the first half of this report show that it is possible to achieve good presynaptic voltage control in the inhibitor during the time window of the F2 component of facilitation. These experimental conditions allow us to explore synaptic facilitation with controlled presynaptic pulses.

Mechanisms of activation

The observation that facilitation can be activated by subthreshold presynaptic pulses does not contradict our current understanding that calcium ions constitute the main driving element of facilitation. In the studies of the squid giant synapse, it was reported that presynaptic I_{Ca} could be detected before any postsynaptic response was observed (Augustine et al. 1985b; Llinás et al. 1981). The subthreshold pulses could, therefore, be triggering a calcium influx that was capable of activating facilitation

but failed to trigger release. This would mean that the calcium binding step that leads to the activation of F2 facilitation had a higher affinity for calcium than that of the secretion process. In the absence of direct measurement of presynaptic calcium concentration, we cannot quantitate the calcium affinity of the activation process. Theoretical estimates of calcium affinity for F1 and F2 facilitation are $\sim 10\text{--}20\ \mu\text{M}$ (Delaney and Tank 1994). This value is consistent with our observation, because it is much lower than the calcium concentration required to trigger release, $100\text{--}200\ \mu\text{M}$ (Adler et al. 1991). Presumably, subthreshold pulses open relatively few channels and the channel opening time is sufficiently brief that local calcium concentration reaches a level of between 20 and $100\ \mu\text{M}$. However, our results cannot rule out the possibility that the calcium binding site for the activation process may have an affinity higher than the 10- to $20\text{-}\mu\text{M}$ range but be located far away from the calcium channels (Wu and Saggau 1994).

The subthreshold activation of the facilitation process can also be partially attributed to the finding that the activation process has a lower calcium cooperativity than that of the secretion process. However, low cooperativity alone cannot account for the saturating nature of the activation curve. Specifically, if the only difference between the secretion and activation processes is their cooperativity, one would expect to see the IPSP_{cod} reach its saturation at a level predicted from the activation curve, by taking the best fit of the activation curve to a higher power. The fact that IPSP_{cod} continues to increase significantly beyond the level at which the activation curve has plateaued suggests that the calcium binding sites of the activation process must have a higher affinity than those of the secretion process. Therefore the subthreshold activation of facilitation could be due to both the low calcium cooperativity and the high calcium affinity of the activation process.

The relationship between F_a and IPSP_{cod} suggests that the calcium cooperativity of the activation of facilitation is lower than that of the secretion process. The main assumption underlying this interpretation is that the amount of transmitter release correlates predominantly with presynaptic I_{Ca} amplitude, regardless of whether I_{Ca} is modulated by changing $[\text{Ca}^{2+}]_o$ or by manipulating the level of depolarization (Augustine and Charlton 1986). Although this generalization is based on a rigorous quantitative analysis, it has only been demonstrated for transmitter release triggered by calcium influx activated during a presynaptic pulse (ON current). Because IPSP peak amplitudes, which are mediated by both ON and tail currents, have been used as an indicator of presynaptic calcium influx in this report, the quantitative relationship between transmitter release and presynaptic tail current should also be considered. This relationship can be inferred from studies of action-potential-mediated transmitter release because it has been suggested that action potentials trigger transmitter release largely by tail current (Augustine 1990; Llinás et al. 1982). Because it has been demonstrated that the $[\text{Ca}^{2+}]_o$ dependence of action-potential-activated transmitter release follows a fourth-power rule (Dodge and Rahamimoff 1967; Stanley 1986) and that the relationship between I_{Ca} and $[\text{Ca}^{2+}]_o$ is linear between 1 and $10\ \text{mM}$ $[\text{Ca}^{2+}]_o$

(Augustine et al. 1985a), it would be reasonable to assume that the dependence of transmitter release on tail current also follows the fourth-power rule. (See Augustine 1990, however, for the situation in which the calcium influx is modulated by action potential duration.) On the basis of these justifications, we used IPSP peak amplitudes as an indicator of a single parameter—the total calcium influx—in this report. However, it should be noted that different amplitudes of presynaptic pulse change both the number of calcium channel openings and single-channel currents. Both parameters contribute to the spatial profile of calcium distribution at a microscopic level. To explore potential contributions of the spatial factors to the activation and detection processes of facilitation, additional experiments would be required in which intracellular distribution of free calcium is modulated by calcium buffer loading (Roberts 1994; Winslow et al. 1994) or by changing $[\text{Ca}^{2+}]_o$.

Assuming a fourth-power calcium dependence of the secretion process, the slope of 0.34 suggests that the activation process should have a cooperativity of between 1 and 2. However, considering the fact that experimental measurement of the calcium cooperativity of the release process often has a value of <4 (Augustine et al. 1985b), the slope can also be interpreted as suggesting a cooperativity of 1. In the absence a quantitative measurement of presynaptic I_{Ca} , we cannot further narrow the range of this estimate and can only conclude that the calcium cooperativity of the activation process is between 1 and 2. Our estimate of the calcium cooperativity of the activation process, therefore, does not directly support results obtained from imaging studies in which the magnitude of short-term synaptic enhancement was found to be linearly related to $[\text{Ca}^{2+}]_i$ (Delaney and Tank 1994; Delaney et al. 1989; Regehr et al. 1994; Wu and Saggau 1994). This linear relationship, at first approximation, would suggest a cooperativity of 1. It is important to point out that the imaging studies measured calcium concentration directly during the decay phase of synaptic enhancement, whereas the estimation of calcium influx by IPSP_{cod} amplitudes deals with the first instant of calcium influx during the activation of facilitation. Therefore the difference in the two experimental conditions may explain the discrepancy between our estimate and that of the imaging studies. Specifically, the calcium influx estimated from IPSP_{cod} may not be linearly related to the level of $[\text{Ca}^{2+}]_i$ several hundred milliseconds later, the point at which measurements were performed in the imaging studies. Alternatively, because the role of calcium in short-term synaptic enhancement is likely to be the driving force for a cascade of biochemical reactions, it is possible that the stoichiometry of the intermediate reactions could account for the difference between our estimate and that of imaging studies.

The experimental approach presented here allows us to reproducibly activate strong facilitation without triggering any transmitter release. This observation by itself is not unique. At the crayfish neuromuscular junction it has been demonstrated that facilitation in the F1 time window still occurred when the conditioning action potential of a paired-pulse protocol probabilistically failed to trigger re-

lease (Dudel and Kuffler 1961; see also Katz and Miledi 1968). The special feature of the voltage control method is that it allows us to gain full control over the extent of presynaptic calcium influx and enable us to consistently activate a high level of facilitation without any transmitter release associated with conditioning stimulation.

Detection of facilitation

The main finding of our detection protocol is that the calcium dependence of facilitated release exhibits a lower calcium cooperativity than that of the secretion process. It is important to note that the detection process is best studied with the use of the presynaptic voltage control method. Although it is possible to approximate the detection protocol with action-potential-based protocols by changing $[Ca^{2+}]_o$, the change of $[Ca^{2+}]_o$ is likely to also change the magnitude of facilitation activated by conditioning action potentials. Keeping both the activation and detection process under strict control is almost impossible when using action-potential-based protocols. Therefore, although there have been previous reports of change in calcium cooperativity of facilitated transmitter release, these studies cannot totally control the complications discussed above (Carlson and Jacklet 1986; Stanley 1986). In addition, these previous studies derived their conclusions from a steady-state stimulation that introduced additional complicating factors such as transmitter depletion and concomitant activation of augmentation and posttetanic potentiation (Magleby 1987; Swandulla et al. 1991). On the other hand, it should be noted that our results were obtained with the use of 5-ms presynaptic pulses, which activate a significantly larger transmitter release than action-potential-like 2-ms pulses (Vyshedskiy and Lin 1997). It is therefore possible that the results described here are not quantitatively applicable to results derived from action-potential-based protocols. Nevertheless, our findings provide new physiological parameters that can be used to provide additional constraints to kinetic models of facilitation.

The slope calculated from the detection protocol was obtained with the use of the maximal level of facilitation that can be activated by 5-ms pulses. Only under such conditions did we obtain a consistent slope in the double logarithm plot. The slope of the double logarithm plot approaches 1 if the magnitude of facilitation is small (data not shown). Depletion of neurotransmitter associated with conditioning stimulation cannot be the cause of the low cooperativity, because the detection protocol was executed with the nonreleasing, subthreshold conditioning stimulation that provides the same D-R coupling plot as that executed by a single suprathreshold conditioning pulse (Fig. 10). Furthermore, the low cooperativity cannot be attributed to saturation of the release mechanism mediated by 5-ms pulses. Because we could record IPSP amplitudes over a range of >1 order of magnitude, one would expect that saturation of transmitter release is minimal for small IPSPs. If saturation were the cause of the low cooperativity, one would then expect the double logarithm plot to exhibit two slopes, with a value close to one at the low end and a shallower slope at the high end. The plot in Fig. 12D does not indicate such a trend. Having eliminated

obvious artifacts, the lower cooperativity would, on appearance, support the classical residual calcium hypothesis for facilitation. Specifically, the classical model assumes that all four calcium binding sites of the secretion step have identical calcium affinity and that residual calcium participates in the facilitation process by binding to one or more of the calcium binding sites. However, calcium imaging studies and mathematical modeling have conclusively ruled out the classical model on quantitative grounds (Delaney and Tank 1994; Delaney et al. 1989; Winslow et al. 1994). Revisions of the classical model have been proposed in which one assigns different calcium affinities to the calcium binding steps of the secretion process (Bertram et al. 1996; Stanley 1986; Yamada and Zucker 1992). The revised models reconcile the calcium imaging data with the basic concept of the classical model. Our observation is also consistent with the revised models. It should be added that the lower cooperativity automatically accounts for the behaviors of F_n and F_a . Specifically, the definition of F_n is the ratio of $IPSP_{test}$ over $IPSP_{cnt}$ minus 1. A lower calcium cooperativity of $IPSP_{test}$ would leave a calcium concentration term in the denominator of the ratio. As test pulse amplitudes increase, the calcium concentration term increases and F_n decreases. Similarly, the rise of F_a can be simplistically associated with increasing calcium concentration activated by test pulses of increasing amplitude.

Although our results support existing mathematical models for facilitation, these models still require a significant conceptual revision to account for one peculiar behavior of facilitation and augmentation. Studies in both frog and crayfish neuromuscular junctions have suggested that the maximal level of facilitation does not occur immediately after the end of conditioning stimulation. Instead, there appears to be a delay in the appearance of the maximum (Bittner 1989; Mallart and Martin 1967; Van der Kloot 1994; unpublished observations). Furthermore, a recent calcium imaging study of hippocampal mossy fiber synapse has shown that the onset of augmentation lags behind the peak of $[Ca^{2+}]_i$ (Regehr et al. 1994). For the revised residual calcium models to account for the delayed maximum, it would be necessary to propose a mechanism in which one of the calcium binding sites of the secretion process that is involved in facilitation requires a long delay before it can be transformed into a facilitated state. This modification, however, constitutes a significant conceptual addition to the mathematical models. It would be equally valid to suggest that the delayed maximum indicates a slow biochemical process that does not involve a specific calcium binding site of the secretion process. For example, it is possible to obtain an apparent third-power cooperativity for facilitated release by assuming that the four calcium binding steps have an identical calcium affinity and that the facilitation process increases the calcium affinities of all four sites by an equal amount (unpublished observations). Other hypotheses for facilitation can, however, be ruled out. For example, the facilitation process could potentially involve an increase in the number of available vesicles without a change in the calcium-dependent kinetics of the release process. However, this model cannot readily generate an apparent low calcium

cooperativity during facilitation. Results reported here can be used to check the kinetic models by modifying parameters related to the duration of presynaptic depolarization.

Molecular mechanisms of facilitation

One of the main difficulties in our current understanding of synaptic facilitation is the unbridged gap between physiological and molecular observations. Physiological studies have emphasized the importance of $[Ca^{2+}]_i$ and have established a quantitative relationship between $[Ca^{2+}]_i$ and the magnitude of synaptic plasticity. This emphasis logically leads to speculation that the calcium-calmodulin-dependent protein kinase II (CAM kinase II) pathway may play a critical role in short-term synaptic plasticity (Lin et al. 1990; Llinás et al. 1991). However, deletion of this kinase in mouse attenuates but does not abolish facilitation (Silva et al. 1992). Furthermore, gene knockout studies of synapsin molecules, one of the main presynaptic substrates of CAM kinase II, yield inconclusive results on the role of the CAM kinase II-synapsin pathway in synaptic facilitation (Rosahl et al. 1995). In addition, blockers of calmodulin or CAM kinase II failed to block short-term synaptic enhancement (Kamiya and Zucker 1994; unpublished observations). These observations force one to consider other calcium-dependent biochemical pathways that may be responsible for synaptic facilitation. One such example would be adenosine 3',5'-cyclic monophosphate (cAMP)-dependent phosphorylation, which may be activated by calcium-calmodulin-dependent adenylate cyclase. Although the importance of the cAMP-dependent pathway has been extensively documented in heterosynaptic facilitation (Hawkins et al. 1993), the role of this pathway in homosynaptic short-term plasticity has been less well understood. The most relevant study so far is the analysis of neuromuscular transmission in *Drosophila* mutants in which the cascade of the cAMP-activated pathway is modified (Dudai 1988). In one case, the cAMP-specific phosphodiesterase II gene was deleted (*duc*) (Byers et al. 1981), and in the second case, the calcium-calmodulin-dependent adenylate cyclase activity was abolished (Livingstone et al. 1984). In addition to profound behavior defects (Dudai 1988), synaptic facilitation at the neuromuscular junction is significantly weakened in both mutants (Zhong and Wu 1991). More importantly, the calcium cooperativity of transmitter release at the *duc* synapse is 3 rather than 4 (Zhong and Wu 1991). Because the *duc* mutant has an elevated level of cAMP, which is presumably responsible for the lowered calcium cooperativity, it is conceivable that the decreased calcium cooperativity during synaptic facilitation could be caused by the same mechanism. In this case, it would be reasonable to propose that the F2 component of synaptic facilitation is mediated by calcium-calmodulin-dependent adenylate cyclase.

Physiological significance of the activation and detection protocols

The observation that F_n and F_a do not remain constant as test pulse amplitude changes provides new insights to the interpretation of results obtained from action-potential-based protocols. It has been demonstrated that a change in $[Ca^{2+}]_o$

(Linder 1974; Zucker 1974) or calcium buffer loading (Winslow et al. 1994) does not change the magnitude of facilitation at the crayfish excitor. The inhibitor exhibits the same characteristics (unpublished observations). These findings do not contradict our results for two reasons. First, these studies used relatively few action potentials to activate facilitation, two in the study by Linder and five in that by Winslow et al. As a result, the magnitude of activated facilitation is low. Under conditions of low facilitation, the slope of the double logarithm plot approaches 1 and a change in F_n would not be expected. Second, the use of the same action-potential-based protocol under different levels of $[Ca^{2+}]_o$ changes both the activation and detection processes simultaneously. Specifically, if one assumes that the decreased transmitter release mediated by conditioning action potentials in low $[Ca^{2+}]_o$ is equivalent to sliding to the left on the $IPSP_{cod}$ curve, there must be a concomitant decrease in the activated facilitation (Fig. 8A; the shift to the left should occur in the lower region of the $IPSP_{cod}$ curve because action potentials activated low levels of release in comparison with 5-ms pulses) (Vysheidskiy and Lin 1997). Meanwhile, a smaller calcium influx in low $[Ca^{2+}]_o$ would be able to detect a higher level of F_n , assuming that the small calcium influx in low $[Ca^{2+}]_o$ is equivalent to small test pulses of the detection process. The activation and detection processes move in opposite directions as one manipulates $[Ca^{2+}]_o$. Both factors reconcile our findings with those derived from action-potential-based protocols. More importantly, our results suggest that a constant F_n under different experimental conditions may be the result of several processes with opposing effects. Furthermore, our results suggest the existence of a functional capability of the crayfish excitor and inhibitor that is able to maintain a constant level of F_n under changing physiological conditions.

In contrast to the crayfish neuromuscular junction, high-output synapses, such as the squid giant synapses and some synapses in vertebrate CNS, typically exhibit a higher F_n as $[Ca^{2+}]_o$ is decreased (Andreasen and Hablitz 1994; Charlton and Bittner 1978; Fleidervish and Gutnick 1995; Schulz et al. 1994; Wilcox and Dichter 1994). Although this finding is traditionally explained in terms of a reduced transmitter depletion in low $[Ca^{2+}]_o$ (Magleby 1987; Zucker 1989), our results suggest that an additional layer of considerations should be added to the existing interpretation. The results reported here are consistent with the behavior of the high-output synapses if one assumes that the activation of facilitation in these synapses is near maximal for the range of $[Ca^{2+}]_o$ tested, i.e., around the plateau region of the activation curve. The higher F_n in low $[Ca^{2+}]_o$ can then be partially attributed to the stronger detection capability of action potential in low $[Ca^{2+}]_o$, i.e., a shift to the left on the F_n curve shown in Fig. 12B. This argument may well be valid because the high-output nature of these synapses could be due to a high density of calcium channels, which is equivalent to operating at the right-hand region of the activation and detection curves under physiological conditions.

Results presented in this report represent the first step in the study of synaptic facilitation with the use of the presynaptic voltage control method. This method provides new physiological measurements that may yield new insights to our understanding of synaptic facilitation.

This work was supported by Boston University fund 20617 and National Institute of Neurological Disorders and Stroke Grant NS-31707 to J.-W. Lin. A. Vyshedskiy is a graduate student at the Department of Biomedical Engineering, Boston University.

Address for reprint requests: J.-W. Lin, Dept. of Biology, Boston University, 5 Cummington St., Boston, MA 02215.

Received 26 September 1996; accepted in final form 10 January 1997.

REFERENCES

- ADLER, E. M., AUGUSTINE, G. J., DUFFY, S. N., AND CHARLTON, M. P. Alien intracellular calcium release chelators attenuate neurotransmitter release at the squid giant synapse. *J. Neurosci.* 11: 1496–1507, 1991.
- ANDREASEN, M. AND HABLITZ, J. J. Paired-pulse facilitation in the dentate gyrus: a patch-clamp study in rat hippocampus in vitro. *J. Neurophysiol.* 72: 326–336, 1994.
- ATWOOD, H. L. AND BITTNER, G. D. Matching of excitatory and inhibitory inputs to crustacean muscle fibers. *J. Neurophysiol.* 34: 157–170, 1970.
- AUGUSTINE, G. J. Regulation of transmitter release at the squid giant synapse by presynaptic delay rectifier potassium current. *J. Physiol. Lond.* 431: 343–364, 1990.
- AUGUSTINE, G. J. AND CHARLTON, M. P. Calcium dependence of presynaptic calcium current and postsynaptic response at the squid giant synapse. *J. Physiol. Lond.* 381: 619–640, 1986.
- AUGUSTINE, G. J., CHARLTON, M. P., AND SMITH, S. J. Calcium entry into voltage-clamped presynaptic terminals of squid. *J. Physiol. Lond.* 367: 143–162, 1985a.
- AUGUSTINE, G. J., CHARLTON, M. P., AND SMITH, S. J. Calcium entry and transmitter release at voltage-clamped nerve terminals of squid. *J. Physiol. Lond.* 367: 163–181, 1985b.
- BALNAVE, R. J. AND GAGE, P. W. Facilitation of transmitter secretion from toad motor nerve terminals during brief trains of action potentials. *J. Physiol. Lond.* 266: 435–451, 1977.
- BERTRAM, R., SHERMAN, A., AND STANLEY, E. F. Single-domain/bound calcium hypothesis of transmitter release and facilitation. *J. Neurophysiol.* 75: 1919–1931, 1996.
- BITTNER, G. D. Synaptic plasticity at the crayfish opener neuromuscular preparation. *J. Neurobiol.* 20: 386–406, 1989.
- BYERS, D., DAVIS, R. L., AND KIGER, J. A. Defect in cyclic AMP phosphodiesterase due to the *dunce* mutation of learning in *Drosophila melanogaster*. *Nature Lond.* 289: 79–81, 1981.
- CARLSON, C. G. AND JACKLET, J. W. The exponent of the calcium power function is reduced during steady-state facilitation in neuron R15 of *Aplysia*. *Brain Res.* 376: 204–207, 1986.
- CHARLTON, M., SMITH, S. J., AND ZUCKER, R. S. Role of presynaptic calcium ions and channels in synaptic facilitation and depression at the squid giant synapse. *J. Physiol. Lond.* 323: 173–193, 1982.
- CHARLTON, M. P. AND BITTNER, G. D. Presynaptic potentials and facilitation of transmitter release in the squid giant synapse. *J. Gen. Physiol.* 72: 487–511, 1978.
- DELANEY, K. R. AND TANK, D. W. A quantitative measurement of the dependence of short-term synaptic enhancement on presynaptic residual calcium. *J. Neurosci.* 14: 5885–5902, 1994.
- DELANEY, K. R., ZUCKER, R. S., AND TANK, D. W. Calcium in motor nerve terminals associated with posttetanic potentiation. *J. Neurosci.* 9: 3558–3567, 1989.
- DODGE, A. AND RAHAMIMOFF, R. Co-operative action of calcium ions in transmitter release at the neuromuscular junction. *J. Physiol. Lond.* 193: 419–432, 1967.
- DUDAI, Y. Neurogenetic dissection of learning and short-term memory in *Drosophila*. *Annu. Rev. Neurosci.* 11: 537–563, 1988.
- DUDEL, J. AND KUFFLER, S. W. Mechanisms of facilitation at the crayfish neuromuscular junction. *J. Physiol. Lond.* 155: 530–542, 1961.
- FLEIDERVISH, I. A. AND GUTNICK, M. J. Paired-pulse facilitation of IPSPs in slices of immature and mature mouse somatosensory neocortex. *J. Neurophysiol.* 73: 2591–2595, 1995.
- HAWKINS, R. D., KANDEL, E. R., AND SIEGELBAUM, S. A. Learning to modulate transmitter release: themes and variations in synaptic plasticity. *Annu. Rev. Neurosci.* 16: 625–665, 1993.
- KAMIYA, H. AND ZUCKER, R. S. Residual Ca^{2+} and short-term synaptic plasticity. *Nature Lond.* 371: 603–606, 1994.
- KATZ, B. AND MILEDI, R. The role of calcium in neuromuscular facilitation. *J. Physiol. Lond.* 195: 481–492, 1968.
- LIN, J.-W., SUGIMORI, M., LINÁS, R. R., MCGUINNESS, T. L., AND GREENGARD, P. Effects of synapsin I and calcium/calmodulin-dependent protein kinase II on spontaneous neurotransmitter release in the squid giant synapse. *Proc. Natl. Acad. Sci. USA* 87: 8257–8261, 1990.
- LINDER, T. M. The accumulative properties of facilitation at crayfish neuromuscular synapses. *J. Physiol. Lond.* 238: 223–234, 1974.
- LIVINGSTONE, M. S., SZIOBER, P. P., AND QUINN, W. G. Loss of calcium/calmodulin responsiveness in adenylate cyclase of *rutabaga*, a *Drosophila* learning mutant. *Cell* 37: 205–215, 1984.
- LINÁS, R., GRUNER, J. A., SUGIMORI, M., MCGUINNESS, T. L., AND GREENGARD, P. Regulation by synapsin I and Ca^{2+} -calmodulin-dependent protein kinase II of the transmitter release in squid giant synapse. *J. Physiol. Lond.* 436: 257–282, 1991.
- LINÁS, R., STEINBERG, I. Z., AND WALTON, K. Relationship between presynaptic calcium current and postsynaptic potential in squid giant synapse. *Biophys. J.* 33: 323–352, 1981.
- LINÁS, R., SUGIMORI, M., AND SIMON, S. M. Transmission by presynaptic spike-like depolarization in the squid giant synapse. *Proc. Natl. Acad. Sci. USA* 79: 2415–2419, 1982.
- MAGLEBY, K. L. *Short-Term Changes in Synaptic Efficacy*. New York: Wiley, 1987, p. 21–56.
- MALLART, A. AND MARTIN, A. R. An analysis of facilitation of transmitter release at the neuromuscular junction of the frog. *J. Physiol. Lond.* 193: 679–694, 1967.
- MARTIN, A. R. A further study of the statistical composition of the endplate potential. *J. Physiol. Lond.* 130: 114–122, 1955.
- MARTIN, A. R. *Junctional Transmission. Presynaptic Mechanisms*. Bethesda, MD: Am. Physiol. Soc., 1977, vol. II, p. 329–355.
- QUASTEL, D. M. AND SAINT, D. A. Transmitter release at mouse motor terminals mediated by temporary accumulation of intracellular barium. *J. Physiol. Lond.* 406: 55–73, 1988.
- REGEHR, W. G., DELANEY, K. R., AND TANK, D. W. The role of presynaptic calcium in short-term enhancement at the hippocampal mossy fiber synapse. *J. Neurosci.* 14: 523–537, 1994.
- ROBERTS, W. M. Localization of calcium signals by a mobile calcium buffer in frog saccular hair cells. *J. Neurosci.* 14: 3246–3262, 1994.
- ROSAHL, T. W., SPILLANE, D., MISSLER, M., HERZ, J., SELIG, D. K., WOLFF, J. R., HAMMER, R. E., MALENKA, R. C., AND SUDHOF, T. C. Essential functions of synapsins I and II in synaptic vesicle regulation. *Nature Lond.* 375: 488–493, 1995.
- SCHULZ, P. E., COOK, E. P., AND JOHNSTON, D. Changes in paired-pulse facilitation suggest presynaptic involvement in long-term potentiation. *J. Neurosci.* 14: 5325–5337, 1994.
- SILVA, A. J., STEVENS, C. F., TONEGAWA, S., AND WONG, Y. Deficient hippocampal long-term potentiation in α -calcium-calmodulin kinase II mutant mice. *Science Wash. DC* 257: 201–206, 1992.
- SIVARAMAKRISHNAN, S., BITTNER, G. D., AND BRODWICK, M. S. Calcium-activated potassium conductance in presynaptic terminals at the crayfish neuromuscular junction. *J. Gen. Physiol.* 98: 1161–1179, 1991a.
- SMITH, S. J., AUGUSTINE, G. J., AND CHARLTON, M. P. Transmission at voltage-clamped giant synapse of the squid: evidence for cooperativity of presynaptic calcium action. *Proc. Natl. Acad. Sci. USA* 82: 622–625, 1985.
- STANLEY, E. F. Decline in calcium cooperativity as the basis of facilitation at the squid giant synapse. *J. Neurosci.* 6: 782–789, 1986.
- SWANDULLA, D., HANS, M., ZIPSER, K., AND AUGUSTINE, G. J. Role of residual calcium in synaptic depression and potentiation: fast and slow calcium signaling in nerve terminals. *Neuron* 7: 915–926, 1991.
- VAN DER KLOOT, W. Facilitation of transmission at the frog neuromuscular junction at 0°C is not maximal at time zero. *J. Neurosci.* 14: 5722–5724, 1994.
- VYSHEDSKIY, A. AND LIN, J.-W. Study of the inhibitor of the crayfish neuromuscular junction by presynaptic voltage control. *J. Neurophysiol.* 77: 103–115, 1997.
- WILCOX, K. S. AND DICHTER, M. A. Paired pulse depression in cultured hippocampal neurons is due to a presynaptic mechanism independent of GABA_B autoreceptor activation. *J. Neurosci.* 14: 1775–1788, 1994.
- WINSLOW, J. L., DUFFY, S. N., AND CHARLTON, M. P. Homosynaptic facilitation of transmitter release in crayfish is not affected by mobile calcium chelators: implications for the residual ionized calcium hypothesis from electrophysiological and computational analysis. *J. Neurophysiol.* 72: 1769–1793, 1994.
- WU, L. G. AND SAGGAU, P. Presynaptic calcium is increased during normal synaptic transmission and paired-pulse facilitation, but not in long-term

- potentiation in area CA1 of hippocampus. *J. Neurosci.* 14: 645–654, 1994.
- YAMADA, M. W. AND ZUCKER, R. S. Time course of transmitter release calculated from stimulations of a calcium diffusion model. *Biophys. J.* 61: 671–682, 1992.
- ZENGEL, J. E. AND MAGLEBY, K. L. Differential effects of Ba^{2+} , Sr^{2+} and Ca^{2+} on stimulation-induced changes in transmitter release at the frog neuromuscular junction. *J. Gen. Physiol.* 76: 175–211, 1980.
- ZHONG, Y. AND WU, C.-F. Altered synaptic plasticity in *Drosophila* memory mutants with a defective cyclic AMP cascade. *Science Wash. DC* 251: 198–201, 1991.
- ZUCKER, R. S. Characteristics of crayfish neuromuscular facilitation and their calcium dependence. *J. Physiol. Lond.* 241: 91–110, 1974.
- ZUCKER, R. S. Short-term synaptic plasticity. *Annu. Rev. Neurosci.* 12: 13–31, 1989.
- ZUCKER, R. S. AND STOCKBRIDGE, N. Presynaptic calcium diffusion and the time courses of transmitter release and synaptic facilitation at the squid giant synapse. *J. Neurosci.* 3: 1263–1269, 1983.